

Signal-Dependent Noise Modelling and Estimation of Optical Imaging Instruments

Massimo Selva, Andrea Garzelli
Department of Information Engineering,
University of Siena,
Via Roma, 56, 53100 Siena, Italy
E-mail: m.selva@ifac.cnr.it, garzelli@dii.unisi.it

Luciano Alparone
Department of Electronics & Telecommunications,
University of Florence,
Via Santa Marta, 3, 50139 Florence, Italy
E-mail: alparone@lci.det.unifi.it

Abstract—This paper deals with an original method to estimate the noise introduced by optical imaging systems, such as CCD cameras, multispectral scanners and imaging spectrometers. The power of the signal-dependent photonic noise is decoupled from the power of the signal-independent noise generated by the electronic circuitry. The method relies on the multivariate regression of local sample statistics such as mean and variance, in which statistically homogeneous pixels produce scatter-points that are clustered along a straight line, whose slope and intercept measure the signal-dependent and signal-independent components of the noise power, respectively. Experimental results carried out on a simulated noisy image and on true data from a modern generation airborne imaging spectrometer highlight the accuracy of the proposed method and its robustness to image textures that may lead to a gross overestimation of the noise, especially for high SNR.

I. INTRODUCTION

Whenever the assumption of additive white Gaussian noise (AWGN) no longer holds, noise modelling and estimation becomes a preliminary task of the most advanced image analysis and interpretation systems. Pre-processing of data acquired with certain modalities, like opto-electronic and coherent, either ultrasound or microwave, may benefit from proper parametric modelling of the dependence of the signal on the noise and from accurate measurements of the noise model parameters.

The knowledge of the noise model parameters is crucial for the task of denoising. LMMSE [1] and especial MAP [2] estimators exhibit a scarce tolerance to mismatches in the parametric noise model.

Recent advances in the technology of opto-electronics imaging devices have lead to the availability of image data, in which the photonic noise contribution may no longer be neglected with respect to the electronic component, which is becoming less and less relevant. As a consequence, pre-processing and analysis methods must be revised or even designed anew to take into account that the noise is signal-dependent. This issue is particularly crucial for optical remote sensing image analysis.

To date, the most powerful noise estimation models are based on multivariate regressions of local statistics [3]. However, the presence of two parametric noise components, e.g. signal-dependent and signal-independent, of comparable power, makes it hard to find a steady solution.

II. SIGNAL-DEPENDENT NOISE MODELLING

A generalised signal-dependent noise model has been proposed to deal with several different acquisition systems. Many types of noise can be described by using the following parametric model [4]

$$\begin{aligned} g(m, n) &= f(m, n) + f(m, n)^\gamma \cdot u(m, n) + w(m, n) \\ &= f(m, n) + v(m, n) + w(m, n) \end{aligned} \quad (1)$$

where (m, n) is the pixel location, $g(m, n)$ the observed noisy image, $f(m, n)$ the noise-free image, modelled as a non-stationary correlated random process, $u(m, n)$ a stationary, zero-mean uncorrelated random process independent of $f(m, n)$ with variance σ_u^2 , and $w(m, n)$ is electronics noise (zero-mean white and Gaussian, with variance σ_w^2). For a great variety of images, this model has been proven to hold for values of the parameter γ such that $|\gamma| \leq 1$. The additive term $v = f^\gamma \cdot u$ is the *generalised signal-dependent* (GSD) noise. Since f is generally non-stationary, the noise v will be non-stationary as well. The term w is the signal-independent noise component and is generally assumed to be Gaussian distributed.

A purely multiplicative noise ($\gamma = 1$) is typical of coherent imaging systems; the majority of de-speckling filters rely on the multiplicative *fully-developed* speckle model [5]. In SAR imagery the thermal noise contribution w is negligible, compared to the speckle term, $f \cdot u$ [6].

A more complex scenario is related to the ultrasonic image generation. Due to the great variability of scatterers size in each tissue, the electronics noise w cannot be neglected. Although a simplified noise model without electronic term and a value of γ in $(0, 1)$, e.g. $\gamma = 1/2$, are accepted as characteristic of this kind of images [7], the presence of the additional term w alleviates for the need of exactly knowing the γ . In fact, if γ is taken to be unity, as for *coherent* noise, an *equivalent signal-dependent* γ may be defined, such that

$$f(m, n) \cdot u(m, n) + w(m, n) \approx f(m, n)^{\gamma_{eq}(f(m, n))} \cdot u_{eq}(m, n). \quad (2)$$

The signal dependent noise in Eq. (2) is the combination of a purely multiplicative term and of a signal-independent term. The outcome exhibits a dependence on the signal that vanishes as $f \rightarrow 0_+$. Whenever $f \cdot u \gg w$, as it happens for SAR

speckle, it stems that $\gamma_{eq}(f) \rightarrow 1_-$. In practice, the left-hand of (2), i.e. (1) with $\gamma = 1$, is taken as a noise model suitable for ultrasonic images [8].

The model (1) is also suitable for *film-grain* noise [9], typical of images obtained by scanning a film (transparent support) or a photographic halftone print (reflecting support). In the former case, $\gamma > 0$ and values $1/3 \leq \gamma \leq 1/2$ are typically encountered; in the latter case, negative values of γ are found [10]. For images obtained from monochrome or colour scanners, the electronics noise w may not be neglected. Its variance is easily measured on a dark acquisition, i.e. when $f = 0$.

Eventually, the model (1) applies also to images produced by opto-electronic devices that acquire natural scenes, such as CCD cameras, multispectral scanners and imaging spectrometers. The latter two are widely used for remote sensing of the Earth, on either airborne or spaceborne platforms. In that case the exponent γ is equal to 0.5. The term $\sqrt{f}u$ stems from the Poisson-distributed number of photons captured by each pixel and is therefore denoted as *photonic* noise. This case will be investigated in the remainder of this paper.

III. OPTO-ELECTRONIC NOISE ESTIMATION

Let us rewrite the model (1) with $\gamma = 0.5$:

$$g(m, n) = f(m, n) + \sqrt{f(m, n)} \cdot u(m, n) + w(m, n). \quad (3)$$

If the variance of (3) is calculated on homogeneous pixels, in which $\sigma_f^2(m, n) = 0$ by definition, thanks to the independence of f , u and w and the fact that both u and w have null mean and are stationary, we can write:

$$\sigma_g^2(m, n) = \sigma_u^2 \cdot \mu_f(m, n) + \sigma_w^2. \quad (4)$$

in which $\mu_f(m, n) \triangleq E[f(m, n)]$ is the non-stationary mean of f . The term $\mu_f(m, n)$ equals $\mu_g(m, n)$, from (3). Eq. (4) represents a straight line in the plane $(x, y) = (\mu_f, \sigma_g^2)$, whose slope and intercept are equal to σ_u^2 and σ_w^2 , respectively. The interpretation of (4) is that on statistically homogeneous pixels the theoretical non-stationary ensemble statistics (mean and variance) of the observed noisy image $g(m, n)$ lie upon a straight line. In practice, homogeneous pixels with $\sigma_f^2(m, n) \equiv 0$ may be extremely rare and theoretical expectation are approximated with local averages. Hence, the most homogeneous pixels in the scene appear in the mean-variance plane to be clustered along the straight line $y = mx + y_0$, in which $m = \sigma_u^2$ and $y_0 = \sigma_w^2$.

The problem of measuring the two parameters of the opto-electronics noise model (3) has been stated to be equivalent to fitting a regression line to the scatter-plot containing homogeneous pixels, or at least the most homogeneous pixels in the scene. The problem is now shifted to detecting the (most) statistically homogeneous pixels in an imaged scene.

One major drawback of the simultaneous estimation of the two parameters of a generic line is that at least two distinct clusters, not necessarily corresponding to two homogeneous image patches, are necessary to yield a steady and balanced line. The procedures developed by some of the authors for

signal-independent noise estimation [3] and SAR speckle estimation [11], once they have been extended to two-parameter noise estimation, have been found to be inadequate for the new task, mainly because the overall noise power, though accurately estimated, was not correctly split into its signal-dependent and independent components.

The new procedure for noise estimation consists either of partitioning the image into blocks or of manually selecting only some regions of interest (ROI). In both cases (unsupervised and semi-supervised), the sequence of blocks/ROIs, “blocks” in the following, is processed in the same way.

From each block the scatter-plot of local 7×7 variance to local 7×7 average is calculated. Since the scatter-plot may contain sparse points due to image textures, only its most clustered points due to the most homogeneous pixels within the image block are retained. This task is achieved by means of an iterative procedure in which the scatter-plot is first split into four quadrants, the most densely populated quadrant is selected and the gravity centre of the cloud of points is calculated. The associated quadratic residues, different along x (mean) and along y (variance) are checked. If both do not exceed a preset *homogeneity* threshold, the gravity centre is accepted and the number of points from which it has been obtained is stored as well. Otherwise each quadrant is split into four sub-quadrants and the procedure is repeated. Convergence is ensured by the fact that the stop thresholds are preliminarily calculated either on homogeneous areas of simulated noisy images, or better on uniform calibration panels placed during the acquisition, whenever possible.

Once the sequence of gravity centres, each with associated the number of points from which it has been generated, has been calculated, such centres are placed in another mean-variance scatter-plane and a two-parameter regression line is fit to the *cloud* of centres. Each centre is weighted by its number of generating points in the calculation of regression coefficients. The slope and intercept of such a straight line are estimates of the two noise parameters.

The main advantage of the above procedure, which may seem to be cumbersome, is that a little homogeneous image block, or better a block containing few statistically homogeneous pixels, not necessarily forming a connected set, yield a gravity centre with low weight, while a block containing many homogeneous points will contribute with a centre having a large weight. The multiplicity of centres will ensure that the regression line is not undetermined, as it would happen in the case of a unique centre, originated from an isotropically spread cloud of dense scatter-points.

IV. RESULTS

The proposed method has been preliminarily validated on simulated noisy images. The widespread test image *Lenna* has been used for this purpose. Noisy versions of *Lenna* with SNR in the interval 5 to 25 dB and equal powers of signal-dependent and signal-independent noise have been generated.

Fig. 1(a) shows the original *Lenna*; Fig. 1(b) its noisy version with SNR = 5 dB. The scatter-plot containing the 64

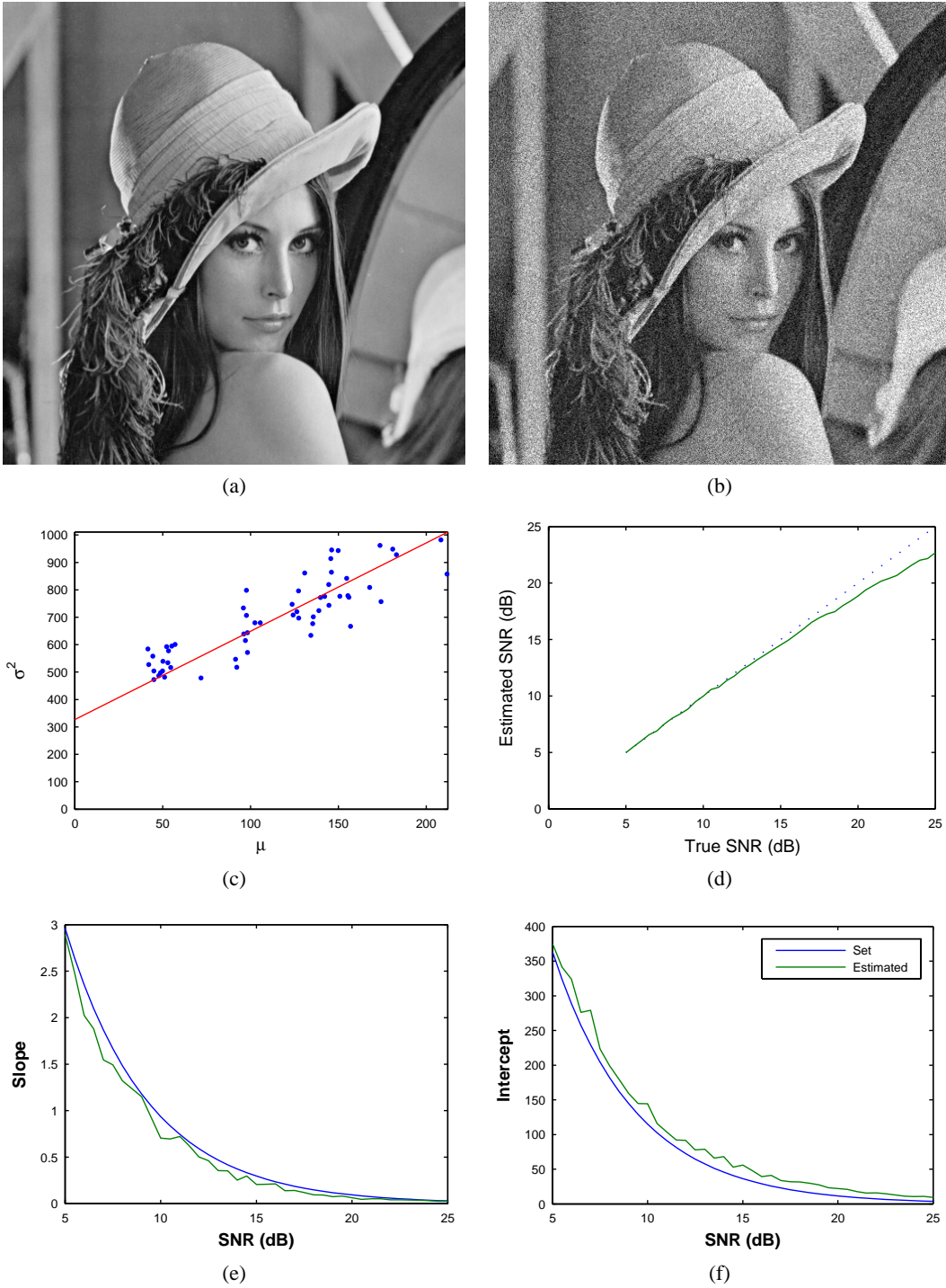


Fig. 1. Test with simulated signal-dependent noise. (a): original *Lenna* image; (b): noisy *Lenna* with SNR = 5 dB and 50% signal-dependent and 50% signal-independent noise powers; (c): scatter-plot of homogeneous areas of (b) with regression line superimposed; (d): estimated SNR vs true SNR (ideal case dotted); (e): estimated (green) and ideal (blue) slope varying with SNR; (f): estimated (green) and ideal (blue) intercept varying with SNR.

gravity centres of the 64 partition blocks of the noisy version in Fig. 1(b) is displayed in Fig. 1(c). True and estimated SNR values are reported in Fig. 1(d). The apparent overestimation of noise at higher SNR is due to the intrinsic noise of the original *Lenna*, whose variance has been measured and found to be about 10. Eventually, the slope and intercept of the estimated regression line are plotted in Figs. 1(e) and 1(f) varying with SNR, each together with the corresponding parameter of the

noise model that has been simulated. This result provides a further insight into the features of the method. The signal-independent noise variance is always slightly overestimated. Conversely, the signal-dependent noise variance, proportional to the slope of the regression line, is always underestimated to a little extent. However, the outcome SNR is balanced and its small drift from the theoretical value (dotted line) depends only on the intrinsic noise of the original test image.

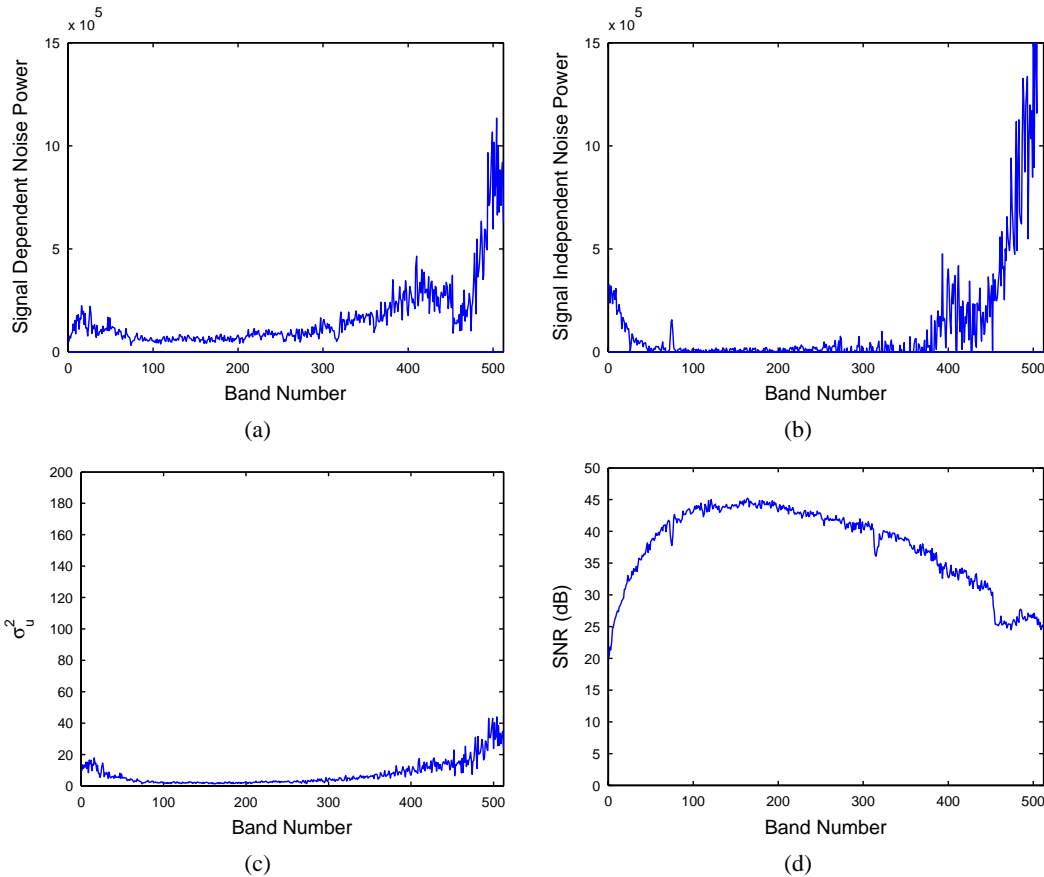


Fig. 2. Test with a true hyperspectral image from an airborne instruments (512 bands in the visible and near-infrared (V-NIR) wavelengths). (a): estimated signal-dependent (photonic) noise power varying with band number; (b): estimated signal-independent (electronic) noise power varying with band number; (c): estimated variance of signal-dependent noise generating term, σ_u^2 varying with band number; (d): estimated SNR varying with band number.

A further experiment was made on the data produced by a modern-generation push-broom imaging spectrometer. A close-range acquisition of the airborne instrument was made with the aid of calibration panels to expedite radiometric and atmospheric corrections. Calibrated radiance data in the visible and near-infrared (V-NIR) wavelengths have been analysed. There are 512 bands in the interval 400 - 1000 nm. The instrument is equipped with a 1024×512 CCD array spanning the across track and spectral direction, respectively. The raw data are acquired with a 12 bit ADC.

Figs. 2(a) and 2(b) show the signal-dependent and signal independent noise powers varying with band number. There is a region in 450 - 850 nm, in which both the noise contributions are approximately constant with the wavelengths. In this interval, the signal-dependent noise is one order of magnitude greater than the signal-independent noise, thereby confirming that the instrument is close to the limits of the photonic noise, which cannot be lowered by improving the electronics. The term σ_u^2 in Fig. 2(c) has a trend with the wavelength flatter than that in Fig. 2(a), since it does not depend on the mean radiance of the scene, which varies with the wavelength. Eventually, SNR is plotted against the band number in Fig. 2(d). All results are in excellent accordance with those measured on calibration panels. However, by measuring means and variances on a unique panel, the two noise contributions cannot be separated.

REFERENCES

- [1] F. Argenti, G. Torricelli, and L. Alparone, "MMSE filtering of generalised signal-dependent noise in spatial and shift-invariant wavelet domains," *Signal Processing*, vol. 86, no. 8, pp. 2056–2066, Aug. 2006.
- [2] F. Argenti, T. Bianchi, and L. Alparone, "Multiresolution MAP despeckling of SAR images based on locally adaptive generalized Gaussian pdf modeling," *IEEE Trans. Image Processing*, vol. 15, no. 11, pp. 3385–3399, Nov. 2006.
- [3] B. Aiazzi, L. Alparone, A. Barducci, S. Baronti, P. Marcoionni, I. Pippi, and M. Selva, "Noise modelling and estimation of hyperspectral data from airborne imaging spectrometers," *Annals of Geophysics*, vol. 49, no. 1, pp. 1–9, Feb. 2006.
- [4] A. K. Jain, *Fundamentals of Digital Image Processing*, Prentice Hall, Engl. Cliffs, NJ, 1989.
- [5] M. Tur, K. C. Chin, and J. W. Goodman, "When is speckle multiplicative?," *Appl. Optics*, vol. 21, no. 7, pp. 1157–1159, Apr. 1982.
- [6] C. Oliver and S. Quegan, *Understanding Synthetic Aperture Radar Images*, Artech House, Boston, MA, 1998.
- [7] T. Loupas, W. N. McDicken, and P. L. Allan, "An adaptive weighted median filter for speckle suppression in medical ultrasonic images," *IEEE Trans. Circuits Syst.*, vol. 36, no. 1, pp. 129–135, 1989.
- [8] F. Argenti and G. Torricelli, "Speckle suppression in ultrasonic images based on undecimated wavelets," *EURASIP J. Appl. Signal Process.*, vol. 2003, no. 5, pp. 470–478, Apr. 2003.
- [9] P. Campisi, J. C. K. Yan, and D. Hatzinakos, "Signal-dependent film grain noise generation using homomorphic adaptive filtering," *IEE P-Vis. Image Sign.*, vol. 147, no. 3, pp. 283–287, June 2000.
- [10] W. K. Pratt, *Digital Image Processing*, J. Wiley & Sons, New York, 1991.
- [11] B. Aiazzi, L. Alparone, S. Baronti, and A. Garzelli, "Coherence estimation from incoherent multilook SAR imagery," *IEEE Trans. Geosci. Remote Sensing*, vol. 41, no. 11, pp. 2531–2539, Nov. 2003.